Calculation of IES Level 3 Flux from Level 2 Counts

T.W. Broiles, P.Mokashi and the IES Team

The Ion and Electron Sensor (IES) uses electrostatic analyzers (ESAs) to differentially measure the energy per charge (E/q) of positively and negatively charged particles. The E/q is measured at 128 different steps from 16 different azimuths and 16 elevations, and if the measured particle mass and charge could be assumed, a velocity space density could also be computed as shown in eq. 1 below. The velocity space density, *f*, is dependent on raw counts from the instrument, C, the speed of measured particles, *v*, the instrument's geometric factor, G, the span of time that particles were counted, Δt, and the instrumental efficiency at which particles were counted, ε. The measured particles speed is inferred from the measured E/q and by estimating the particle's mass, m, and charge, q.

$$f = \frac{2^{C}/_{\Delta t}}{v^4 * G * \epsilon} \quad (1)$$

$$v = \sqrt{\frac{2*(^{E}/_{q})*q}{m}} \quad (2)$$

Unfortunately, cometary ions range from H^+ (1 amu) to CO_2^+ (44 amu) in mass, and while most are singly charged, it may not always be the case. In contrast, cometary negative charged particles are much more likely to electrons, but in at least one case negative hydrogen was observed [Burch et al., 2015]. Consequently, *v* and *f* can vary significantly depending on which species is thought observed.

Our approach to the IES level 3 data product is to distill the level 2 data into its most useful form without making assumptions about the measured particles. Our conclusion from the above discussion is to exclude data dependencies on *v* and leave that to the analysis of future users of the IES data. Therefore, the highest order data product that we can produce is differential flux, DF. We define DF in equation 3 below. Differential flux is computed similarly to velocity space density, with the exception that all dependence on *v* is removed and background signals caused by penetrating radiation and electronic thermal noise are subtracted from the raw counts to define C/Δt'.

$$DF = \frac{^{C}/_{\Delta t'}}{G * \epsilon} \quad (3)$$

Our approach to computing each independent variable in equation 3 will be explained in detail in an upcoming paper [Broiles et al., in preparation], but we will briefly explain each below.

In order to compute C/Δt', we must first identify background noise sources. We consider IES' background noise to be relatively small and uniform across energies and directions because it is caused by penetrating radiation and thermal electronic noise. Therefore, we can isolate this signal by looking at data points where we anticipate no real counts. For both the ion sensor and the electron sensor this can be found in directions where there are complete spacecraft blockages. We average data at high energies, in directions with complete spacecraft blockages for each measurement cycle (electrons: Anode 14, elevation step 0, energies greater than 500 eV; ions: Anode 1, elevation step 16, all energies), and subsequently use a rolling average over the adjacent 10 background estimates to smooth the effect of statistical fluctuations in measured background. This approach still allows the background to vary over longer timescales, and removes variable timescale radiation sources such as interplanetary coronal mass ejections and solar flares. Once we have an estimate for the background, it is subtracted from the raw counts to compute C/Δt'.

The geometric factor used here for ions is equivalent to the value described in the IES instrument paper [Burch et al., 2007]. However, for the electron sensor a more precise estimate was computed using flight data from Jan. 1, 2015. Based on previous cometary electron observations Zwickl et al. [1986] found that electrons were isotropically distributed in the rest frame to first order. We summed all of the counts over time to produce a single measurement for each direction and energy for the entire day's data. We then assumed that one direction of the instrument had the ideal geometric factor as described by the Burch et al. [2007] paper. We chose a direction that was generally Sunward point, free of spacecraft blockages, and had minimal deflection voltage applied (Anode 3, elevation step 9). We compare the observed counts at every look-direction to that of our ideal direction at each energy step. Equation 4 describes our method for calculating the calibrated geometric factor, G', using observed counts summed over time, C, at each azimuth step, i, elevation step, j, energy step, k, and the published geometric factor, G [Burch et al., 2007].

$$G'_{i,j,k} = \frac{C_{i,j,k}}{C_{3,9,k}} G \tag{4}$$

Equations 5 and 6 describe our estimate of the uncertainty G' using error propagation of equation 1. Uncertainty in $C_{i,j,k}$ is estimated with Poisson statistics, and G is treated as a known constant. Covariance between counts at azimuth i and elevation j, and azimuth 3 and elevation 9, $\sigma_{ij,39,k}$, is estimated using the series of data that is integrated to calculate $C_{i,j,k}$.

$$\Delta G'^{2}_{i,j,k} = \sigma^2_{i,j,k} \left(\frac{\partial G'_{i,j,k}}{\partial C_{i,j,k}}\right)^2 + \sigma^2_{3,9,k} \left(\frac{\partial G'_{i,j,k}}{\partial C_{3,9,k}}\right)^2 + 2\sigma_{ij,39,k} \left(\frac{\partial^2 G'_{i,j,k}}{\partial C_{i,j,k} \partial C_{3,9,k}}\right) \tag{5}$$

$$\Delta G'^{2}_{i,j,k} = \left(\frac{C_{i,j,k}}{C^2_{3,9,k}} + \frac{C^2_{i,j,k}}{C^3_{3,9,k}} - \frac{2\sigma_{ij,39,k}}{C^2_{3,9,k}}\right) G^2 \tag{6}$$

Figure 1 shows a comparison of IES flux observations with the application of a constant geometric factor (Figures 1a, 1b) and the new, flight-calibrated geometric factor

(Figures 1c, 1d). Panels on the left contain spectrograms of electron flux summed over energy with azimuths along the abscissa and elevations along the ordinate. Right panels show spectrograms of electron flux summed over all elevations, in a polar coordinate system where energy is the radial direction and azimuth is the azimuthal direction. The bottom panels using the flight calibrated geometric factor have more isotropic flux.

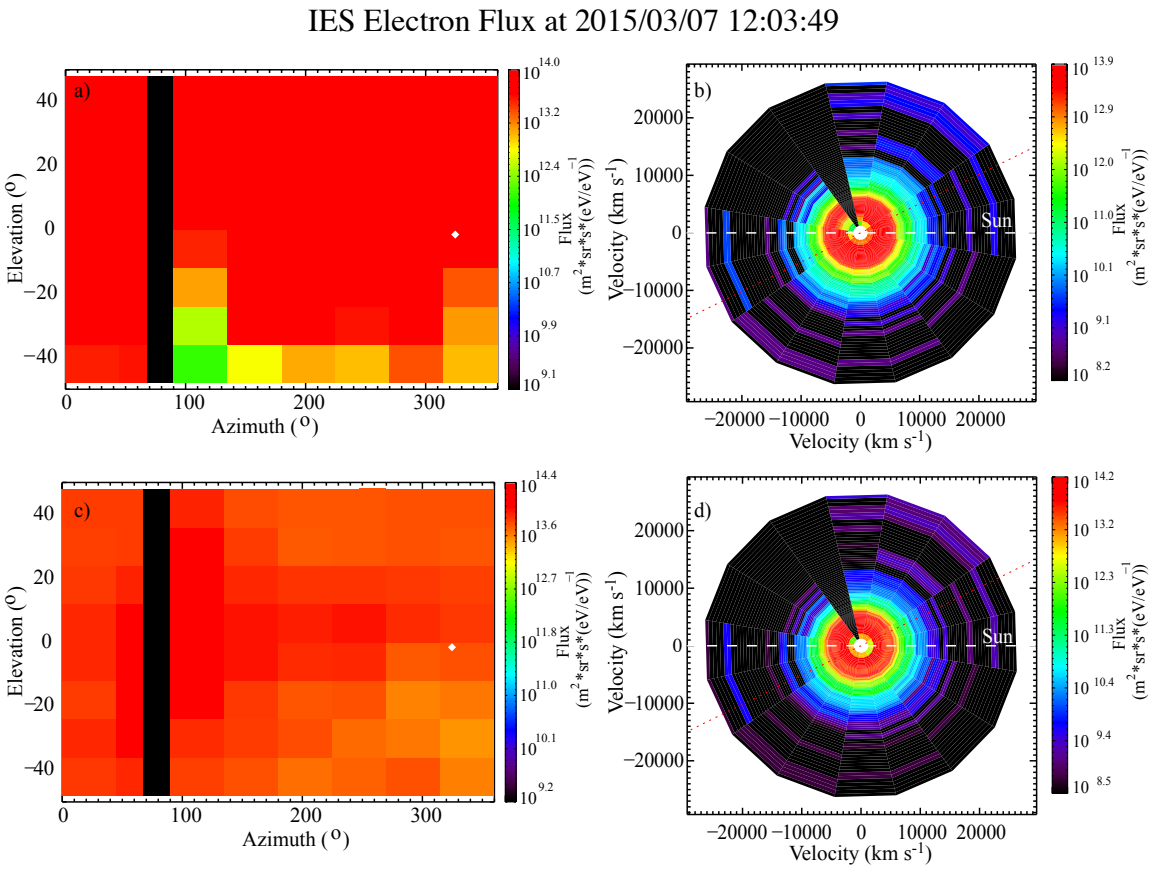

Figure 1: A comparison of the observed differential flux assuming a flat geometric factor (top panels), and assuming our flight calibrated geometric factor (bottom panels). Left panels show differential flux for a singal measurement cycle summed over all energies. Right panels show differential flux for a single measurement cycle summed over all elevations.

The value of Δt is instrument mode specific, but is 1 of 4 values depending on the measurement cycle length. Table 1 links each value of Δt to the cycle length.

Table 1: A table of values for Δt relative to measurement cycle length.

Measurement cycle length (seconds)	Δt (seconds)
128	0.032
192	0.095
256	0.095
512	0.22
768	0.47

1024	0.47

The instrument efficiency is energy dependent, and determined by the efficiency of IES' micro-channel plates (MCPs) to count an incident particle. This efficiency was estimated from Kurz et al. [1979]. The data from that paper was fit with a 5 coefficient Gaussian relative to log of the incident particle's energy. Figure 2 shows the results of that fit for electrons. We elected to compute instrument efficiency in this way rather than using a simpler look up table, because each mode averages our energy steps differently. This approach allows us to quickly compute the instrument efficiency by simply knowing the average energy of a measurement. However, this does have one draw back in that we assumed particles were singly charged, but this is almost certainly the case with the exception of solar wind α particles.

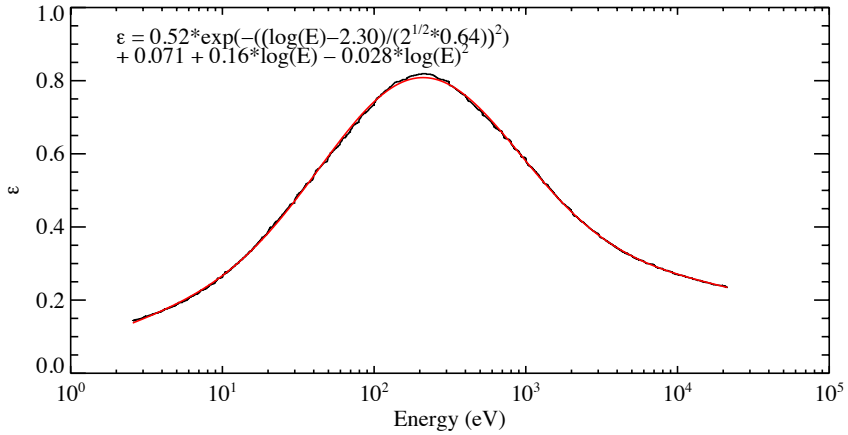

Figure 2: The relationship between MCP efficiency and incident electron energy. Black curve shows data from Kurz et al. [1979], Red curve shows our empirical fit.

The exact equations used to compute efficiency for both ions and electrons are shown below in eqs. 7 and 8. We also note that ions experience a post-acceleration after the ESA, which adds an additional 2000 eV to particle before they hit the MCP. We account for this by adding that energy to E before computing efficiency. Electrons have a much smaller post-acceleration of 37 eV, which is also accounted for in our analysis.

$$\epsilon_{ions} = 0.55e^{-\left(\frac{\log E - 4.26}{\sqrt{2}*0.57}\right)^2} + 0.015 * \log^2 E - 0.11 \log E + 0.29 \quad (7)$$

$$\epsilon_{electrons} = 0.52e^{-\left(\frac{\log E - 2.30}{\sqrt{2}*0.64}\right)^2} - 0.028 * \log^2 E + 0.\rho\varphi \log \quad E + 0.071 \quad (8)$$

Examples

For example, IES might observe 100 counts in a particular direction during a single 1024 s ion measurement at 100 eV, with a background count level of 0.2 counts. Equation 9 replaces the variables in eq. 3 with the above-mentioned values to show the resulting differential flux.

$$\epsilon_{ions} = 0.55e^{-\left(\frac{\log(2000+100)-4.26}{\sqrt{2}*0.57}\right)^2} + 0.015\log^2(2000+100) - 0.11\log(2000+100) + 0.29 \approx 0.55$$

$$DF = \frac{{}^{100\,(C)}/_{0.47(s)} - {}^{0.2\,(C)}/_{0.47(s)}}{6*10^{-9}\left({}^{m^2*sr*eV}/_{\left(eV\frac{counts}{ion}\right)}\right)*0.55} = 6.435*10^{10}\left(\frac{ions}{m^2*s*sr*({}^{eV}/_{eV})}\right) \quad (9)$$

Eq. 10 repeats the example shown in eq. 9, but for a 256 s electron measurement at 20 eV with an approximated geometric factor value of $2.8*10^{-9}$. 15 counts were observed with an estimated background of 0.3 counts.

$$\epsilon_{electrons} = 0.52e^{-\left(\frac{\log(20+\sigma\chi)\wr 2\backepsilon\sigma}{\sqrt{2}*0.64}\right)^2} - 0.028\log^2(20+\sigma\chi) + 0.\rho\varphi\grave{\imath}\log\ 20\text{ش}\sigma\chi + 0.071 \approx 0.6\varsigma\upsilon$$

$$DF = \frac{{}^{15\,(C)}/_{0.095(s)} - {}^{0.3\,(C)}/_{0.095(s)}}{2.8*10^{-9}\left({}^{m^2*sr*eV}/_{\left(eV\frac{counts}{electron}\right)}\right)*0.6\varsigma\upsilon} = 8.\psi\tau\,\varsigma\varepsilon\rho 0^{10}\ \left(\frac{electrons}{m^2*s*sr*({}^{eV}/_{eV})}\right) \quad (10)$$

References

Broiles, T.W. et al., Characterizing cometary electrons with kappa distributions, *Journal of Geophysical Review-Space Science*, in preperation

Burch, J. L., R. Goldstein, T. E. Cravens, W. C. Gibson, R. N. Lundin, C. J. Pollock, J. D. Winningham, and D. T. Young (2007), RPC-IES: The Ion and Electron Sensor of the Rosetta Plasma Consortium, *Space Sci Rev*, *128*(1-4), 697–712, doi:10.1007/s11214-006-9002-4.

Burch, J. L., T. E. Cravens, K. Llera, R. Goldstein, P. Mokashi, C.-Y. Tzou, and T. Broiles (2015), Charge exchange in cometary coma: Discovery of H- ions in the solar wind close to comet 67P/Churyumov-Gerasimenko, *Geophysical Research Letters*, *42*(13), 5125–5131.

Kurz, E. A. (1979). Channel electron multipliers, *American Laboratory*, *11*(3), 67.

Zwickl, R. D., D. N. Baker, S. J. Bame, W. C. Feldman, S. A. Fuselier, W. F. Huebner, D. J. McComas, and D. T. Young (1986), Three Component Plasma Electron Distribution in the Intermediate Ionized Coma of Comet Giacobini-Zinner, *Geophys. Res. Lett.; (United States)*, *13:4*.